Communication

Reversible Intramolecular C#C Bond Formation/Breaking and Color Switching Mediated by a N,C-Chelate in (2-ph-py)BMes and (5-BMes-2-ph-py)BMes

Ying-Li Rao, Hazem Amarne, Shu-Bin Zhao, Theresa M. McCormick, Sanela Martic#, Yi Sun, Rui-Yao Wang, and Suning Wang

J. Am. Chem. Soc., **2008**, 130 (39), 12898-12900 • DOI: 10.1021/ja8052046 • Publication Date (Web): 04 September 2008

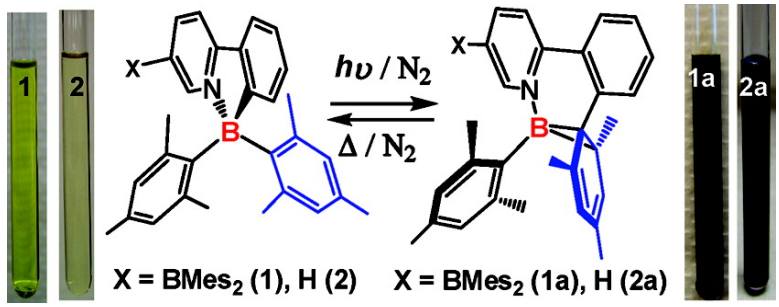

More About This Article

Additional resources and features associated with this article are available within the HTML version:

- Supporting Information
- Access to high resolution figures
- Links to articles and content related to this article
- Copyright permission to reproduce figures and/or text from this article

View the Full Text HTML

J|A|C|S
COMMUNICATIONS

Published on Web 09/04/2008

Reversible Intramolecular C−C Bond Formation/Breaking and Color Switching Mediated by a N,C-Chelate in (2-ph-py)$BMes_2$ and (5-$BMes_2$-2-ph-py)$BMes_2$

Ying-Li Rao, Hazem Amarne, Shu-Bin Zhao, Theresa M. McCormick, Sanela Martić, Yi Sun, Rui-Yao Wang, and Suning Wang*

Department of Chemistry, Queen's University, Kingston, Ontario, K7L 3N6, Canada

Received April 15, 2008; E-mail: wangs@chem.queensu.ca

Organoboron compounds with a conjugate chromophore have gained popularity for applications in optoelectronic materials and devices.[1] Based on the geometry of the boron center, there are two classes of organoboron compounds—trigonal planar and tetrahedral. Despite both types of organoborons having been investigated extensively for use as charge transport materials and emitters in organic devices,[2,3] hybrid molecules that contain both 3- and 4-coordinate triarylboron groups are previously unknown. To examine and exploit the photophysical properties of such hybrid boron compounds, we synthesized a new diboron molecule (5-$BMes_2$-2-ph-py)$BMes_2$ (**1**). To determine the impact of the trigonal boron center on the properties of **1**, we also synthesized the monoboron analogue (2-ph-py)$BMes_2$ (**2**). Our investigation on these two molecules revealed a rare phenomenon: a reversible intramolecular C−C bond formation/breaking process involving a tetrahedral B center, accompanied by a distinct color switching, as shown in Scheme 1. In view of the potential implications/applications of the new findings on the use of organoboron materials in optoelectronic devices and organic syntheses, the preliminary results of our investigation are reported herein.

Scheme 1. Transformation of **1** and **2**

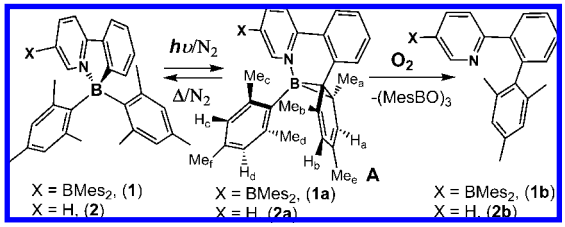

The structures of **1** and **2** were determined by X-ray diffraction analyses with **1** shown in Figure 1. The B−C bond lengths around the tetrahedral B center in **1** and **2** are similar (1.628(6)−1.666(6) Å) but much longer than those around the trigonal B center (1.554(6)−1.588(6) Å) in **1**. The B−N bonds length in **1** and **2** (1.636(5), 1.653(2) Å, respectively) are normal for tetrahedral boron molecules.[3] Both compounds display distinct luminescence (Figure 2) with λ_{max} = 525 nm, $\Phi > 0.3$ for **1** and λ_{max} = 480 nm, $\Phi \approx 0.1$ for **2**. DFT calculations indicate that the lowest electronic transition for both compounds is charge transfer from the mesityls of the tetrahedral boron to the Mes_2B-py-ph in **1** and the py-ph chelate in **2** (see Supporting Information, S8.1). Compound **1** displays a reversible reduction peak, characteristic of a triarylboron,[2] at −1.88 V (vs $FeCp_2^{0/+}$ in DMF) while **2** has an irreversible reduction peak at −2.35 V, corresponding to a LUMO energy level of −2.92 and −2.45 eV for **1** and **2**, respectively. Hence, the hybrid diboron molecule **1** appears to be better than the monoboron **2** in terms of electron accepting ability and emission efficiency. However, both molecules were found to be very sensitive toward light.

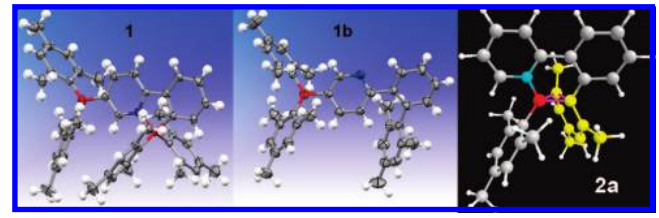

Figure 1. (Left) Crystal structures of **1** and **1b** with 50% thermal ellipsoids: red, B; blue, N. (Right) Structure **2a** calculated by DFT.

When irradiated by UV light (365 nm) under N_2 in toluene, **1** becomes dark olive green and **2** becomes dark navy blue, accompanied by a rapid loss of fluorescence (Figure 2). The UV−vis spectrum of **1** shows a new broad band covering the entire 400−900 nm region with λ_{max} at 431, 523, and 714 nm (ε = 6192, 2864, 3032 M^{-1} cm^{-1}) appearing and gaining intensity with the exposure time. Similarly, an intense broad band with λ_{max} = 599 nm (ε = 5028 M^{-1} cm^{-1}) appears and grows rapidly in the spectrum of **2**. The dark olive green and dark blue solutions obtained from irradiation are ESR silent at 298 and 77 K, thus ruling out the presence of radical species. The structural origin of the drastic color change of **1** and **2** was investigated by NMR.

Upon irradiation at 365 nm, the ^{1}H NMR spectra of **1** and **2** display a new set of well-resolved peaks belonging to a single entity, designated as **1a** and **2a**, respectively, that grow with the exposure time while the peaks of **1** and **2** diminish, as shown in Figure 3 (see S5.1 for the spectra of **1** to **1a** conversion). The conversion rate of **2** to **2a** is about twice that of **1** to **1a**. Extended irradiation converts **1** and **2** to **1a** and **2a** completely, respectively. The most revealing features in the NMR spectra are the chemical shift (δ)

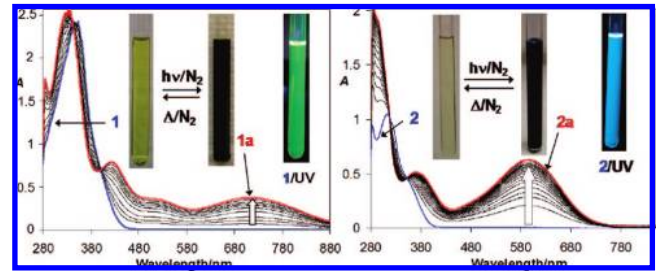

Figure 2. UV−vis spectra of **1** and **2** recorded under N_2 in toluene (1.25×10^{-4} M) with ~10 s intervals of light exposure (365 nm) for **1** and ~5 s intervals for **2**. (Inset, left) Photographs of **1** and **2** showing the color switch before and after irradiation; (right) photographs of the fresh solutions of **1** and **2** under UV light, showing their emission colors.

10.1021/ja8052046 CCC: $40.75

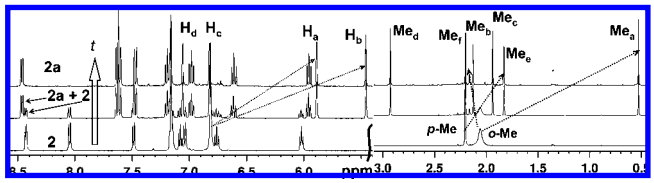

Figure 3. ^{1}H NMR spectra for conversion of **2** to **2a** in C_6D_6 at 298 K after irradiation at 365 nm. Peak assignments are for the blue enantiomer in Figure 4. Dashed arrows indicate the δ change of the mesityl ring.

change of the mesityls on the tetrahedral B center in both compounds, as shown in Figure 3. All methyls and all aryl H atoms on the two mesityls in **2a** have distinct chemical shifts, indicative of the presence of a restricted rotation around the B−C_{Mes} bonds. One of the mesityls shows upfield shift by its aryl H atoms (H_a and H_b) and one of its ortho-methyls (Me_a). The chemical shift at 0.55 ppm by Me_a is consistent with its attachment to a sp^3 carbon, not a sp^2 one. Similar features are also observed in the spectrum of **1a**. ^{11}B NMR shows that the ^{11}B signal of the tetrahdral B center in **1** and **2** (4.90 ppm, **1**; 5.02 ppm, **2**) shifts to −9.65 ppm in **1a** and −9.91 ppm in **2a**, indicative of the retention of the tetrahedral geometry.[3,4a] The complete ^{1}H and ^{13}C NMR spectral assignments for **1a** and **2a** are achieved using COSY, HMBC,[4b] and NOESY NMR data and the structural model obtained by DFT calculations, which enable us to conclude that **1a** and **2a** have the borabicyclo-[4.1.0]hepta-2,4-diene structure **A** in Scheme 1, where a C−C bond is formed between the phenyl and one of the mesityls. Structure **A** shares some common features with the dark red species **B** shown in Chart 1, reported by Schuster et al.,[5] including the distinct upfield shift by H′ compared to H (for R = R′ = Ph, H at 5.55 and H′ at 1.39 ppm) and the intense low energy absorption band at ∼510 nm, which are not known for the related borepin isomers.[6,7] Although **B** and its analogues have often been suggested as precursors to borepins or vice versa,[6] we did not see any evidence for borepin (**2c**) formation in our system. We ruled out the borepin structure for **2a** based on the observation of correlation peaks between C_x and H_a, C_x and Me_a in the HMBC[4b] spectrum of **2a** (Figure 4) that is consistent with the presence of a C_x-C_y bond and the structure **A**. Furthermore, the ^{13}C chemical shifts of the quaternary C_x and C_y atoms (46.00 and 29.48 ppm) are in the aliphatic not the aromatic region, in contrast to those reported for trigonal-planar or tetrahedral borepins,[6,7] which again agrees with the structure **A**. The same is true for **1a** (see S1.3 and S 5.4−5.5).

Chart 1

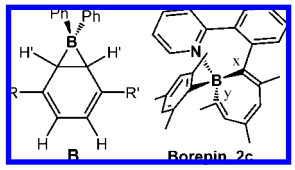

The calculated structure of **2a** shows that the six-membered chelate ring is planar and nearly perpendicular to the BCC ring and the C_{ph}−C_{Mes} distance is 1.48 Å, while the bond lengths within the BCC ring are 1.66, 1.63 Å (B−C), 1.56 Å (C−C). **2a** is clearly more congested than **2**, evidenced by the short separation distances between the mesityl and the cyclohexadienyl, consistent with the restricted rotation of the mesityl in **1a** and **2a** revealed by ^{1}H NMR. A strong NOE cross peak between H_a and Me_d in the NOESY spectra of **1a** and **2a** (see S5.6−5.7) agrees well with the short spatial separation distance between H_a and Me_d (∼2.6 Å) in **2a**. The bulky trigonal $BMes_2$ group in **1** clearly destabilizes the

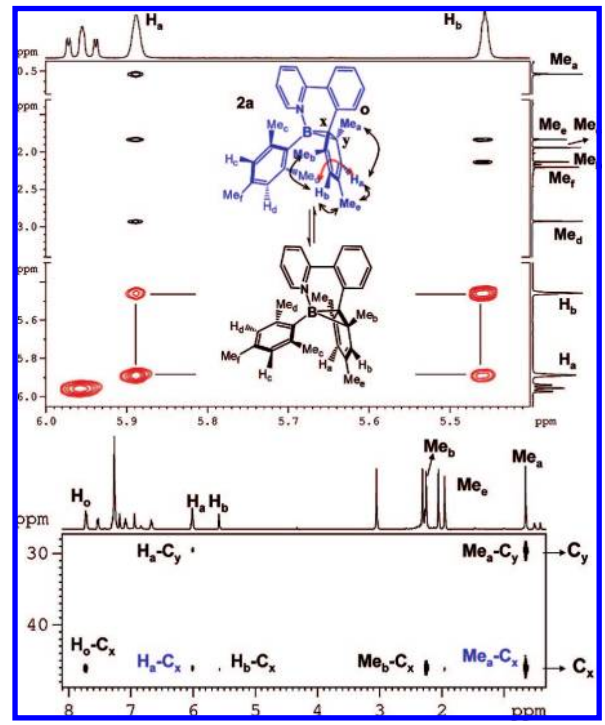

Figure 4. (Top) Portions of the ^{1}H NOESY spectrum of **2a** at 298 K in C_6D_6 showing the exchange cross-peak H_a↔H_b (red) and their NOE cross-peaks (black) with methyls. (Bottom) A partial HMBC spectrum of **2a** in C_6D_6 at 283 K showing H_a, Me_a, and C_x correlation peaks.

transition state, hence resulting in the slower conversion of **1** to **1a**, relative to that of **2** to **2a**. Interestingly, the NOESY spectra also display strong chemical exchange cross peaks of H_a ↔ H_b, Me_a ↔ Me_b on the cyclohexadienyl ring, and H_c ↔ H_d, Me_c ↔ Me_d on the mesityl for both **1a** and **2a**, indicative of the presence of slow enantiomer interconversion in solution via the B−C bond migration (Figure 4). The T_c for any of the exchange pairs in the 1D NMR spectra could not be determined because of the rapid thermal reversal of **1a** and **2a** back to **1** and **2** at high temperatures. Nonetheless, the lower limit of the activation barrier for the racemization was estimated to be >16 kcal/mol for both.[4c]

DFT calculations established that the HOMO level of **2a** is dominated by the cyclohexyldienyl and the boron atom while the LUMO level is a π^* orbital involving mostly the ph-py ring. The intense and dark colors of **1a** and **2a** can be explained by a low energy charge transfer transition from the B-cyclohexadienyl to the $B(Mes)_2$-py-ph and the py-Ph moiety, respectively. TDDFT calculations on **2a** confirmed that the calculated UV−vis spectrum has the same pattern as the experimental one (see S8.2), further supporting the structure **A** for **2a**. The HOMO−LUMO gap of **2a** is 1.14 eV less than that of **2**, consistent with the difference of the optical energy gaps obtained from UV−vis spectra. The Lewis acidic trigonal B center in **1a** stabilizes the π^* level of the py-ph group, thus lowering the transition energy compared to **2a**, resulting in the color distinction between the two. Because the lowest electronic transition in **1** and **2** is charge transfer from the mesityls of the tetrahedral B to the N,C-chelate, photoisomerization to **1a** and **2a** is most likely initiated by a photoinduced internal electron transfer.

Most remarkable is the reversibility of the **1** to **1a** and **2** to **2a** transformations under nitrogen. The dark blue **2a** can be fully converted back to the colorless **2** after heating in C_6D_6 in the dark. ^{1}H and ^{11}B NMR experiments confirmed that the thermal reversal of **1a** and **2a** back to **1** and **2** is quantitative. The ^{11}B NMR spectra for the photoisomerization and the thermal reversal cycle of **2**→**2a**→**2** are

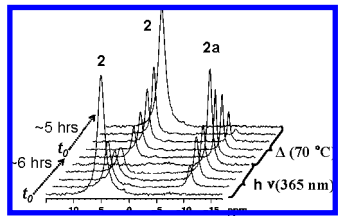

Figure 5. ^{11}B NMR spectra for the photoisomerization of **2** to **2a** in C_6D_6 at 365 nm, 25 °C, and the thermal reversal of **2a** to **2** at 70 °C.

shown in Figure 5. At 323 K, $t_{1/2}$ is ~84 min for **1a** and ~462 min for **2a**. The activation energies for the thermal reversal of **1a** and **2a** were determined to be 107 and 110 kJ/mol, respectively. The much faster reversal by **1a**, relative to **2a**, is consistent with greater steric congestion that destabilizes the molecule.

Irreversible photoisomerization involving a tetrahedral borane and a C−C bond formation is previously known.[5,6d] For example, Schuster et al. reported[5] that the anion $\{B(p\text{-biphenyl})Ph_3\}^-$, upon irradiation at 254 nm, forms the dark red borate species **B** (ref 5, Chart 1, R = R′= Ph). The mechanism of **1a** and **2a** formation is likely similar to that of **B**. However, the **B**-like structure was not observed in our system, which can be attributed to the internal py group that prevents the boron center from migrating to the *meta*-carbon. Most significant is that **B** and analogues do not undergo thermal reversal.[5,6d] The facile thermal reversal of **1a** and **2a** to **1** and **2** by breaking a C−C bond is unprecedented for organoboron compounds, which, we believe, is facilitated by the internal 2-py group that holds the B center and the aryl groups in place, thus making the reversible C−C bond formation and breaking possible. Interestingly, a reversible photo–thermal color switching similar to that in the solution was also observed for **1**- or **2**-doped PMMA films under N_2, indicating that the reversible C−C bond breaking/formation of **1** and **2** also occurs in the solid state (see S5.3a).

1a and **2a** are highly reactive toward oxygen. When exposed to O_2, the deep colored **1a** and **2a** are converted to the colorless species **1b** and **2b** instantaneously and quantitatively as established by NMR. This reactivity of **1a** and **2a** is reminiscent of the formation of a *p*-diphenylbenzene from the O_2 oxidation of **B**.[5] **1b** and **2b** were isolated and fully characterized. The structure of **1b** determined by X-ray diffraction is shown in Figure 1, which confirms that the trigonal $BMes_2$ group in **1** can survive the photo-oxidation process. **1b** and **2b** no longer contain the tetrahedral B center, which was eliminated as $(MesBO)_3$, based on NMR and MS evidence. **1** and **2** can also be converted directly to **1b** and **2b** via the **1a** and **2a** intermediates by reacting with O_2 under light. At 365 nm and 25 °C, the $t_{1/2}$ for **1** to **1b** and **2** to **2b** conversion was determined to be ~24 min and ~9 min, respectively, which correlate well with the relatively faster conversion rate of **2** to **2a**, compared to **1** to **1a**. It must be emphasized, however, that under ambient light and temperature, the photoisomerization and photo-oxidation of **1** are faster than those of **2** ($t_{1/2}$ of photo-oxidation = ~39 min for **1**, ~3.2 h for **2**), because of the lack of absorption in the visible region by **2** (Figure 2). Hence, albeit providing a greater stability toward UV light due to the greater steric hindrance, the trigonal $BMes_2$ group decreases the HOMO−LUMO gap in **1** to the visible region, hence lowering its stability toward ambient light, compared to **2**.

In summary, a reversible isomerization process involving a tetrahedral B center and the formation/breaking of a C−C bond and color switching has been established. Although many organic photochromic systems are known,[8] **1** and **2** are the first examples of organoborons that display reversible photo–thermal color switching. The N,C-chelates in both compounds play a key role in mediating the isomerization process. The high susceptibility of **1** and **2** toward oxygen under light will limit the use of this class of materials in certain optoelectronic devices. However, the facile reversible C−C bond formation/breaking process may be exploited for organoboron-assisted organic syntheses. Further investigation is underway to systematically examine the effects of steric and electronic factors of different N,C-chelates on the photochemical stability and the reactivity of four-coordinate organoboron compounds.

Acknowledgment. We thank the Natural Sciences and Engineering Research Council of Canada for financial support, Peter Wan for his valuable insight on organoboron photochemistry, Bruce Hill for his help in ESR experiments, and Gang Wu and Francoise Sauriol for their assistance in 2D NMR.

Supporting Information Available: Experimental and characterization details for all compounds; UV−vis and fluorescent spectra, 1D (^{1}H and ^{13}C) and 2D (HMBC, COSY, NOESY) NMR and kinetic data, HH crystal data of **1**, **2**, and **1b**, DFT and TD-DFT calculation details for **1**, **2**, and **2a**. This material is available free of charge via the Internet at http://pubs.acs.org.

References

(1) (a) Yamaguchi, S.; Wakamiya, A. *Pure Appl. Chem.* **2006**, *78*, 1413. (b) Yamaguchi, S.; Shirasaka, T.; Akiyama, S.; Tamao, K. *J. Am. Chem. Soc.* **2002**, *124*, 8816. (c) Yamaguchi, S.; Akiyama, S.; Tamao, K. *J. Am. Chem. Soc.* **2001**, *123*, 11372. (d) Entwistle, C. D.; Marder, T. B. *Angew. Chem., Int. Ed.* **2002**, *41*, 2927. (e) Entwistle, C. D.; Marder, T. B. *Chem. Mater.* **2004**, *16*, 4574. (f) Chiu, C. W.; Gabbai, F. P. *J. Am. Chem. Soc.* **2006**, *128*, 14248. (g) Hudnall, T. W.; Melaimi, M.; Gabbai, F. P. *Org. Lett.* **2006**, *8*, 2747. (h) Lee, M. H.; Agou, T.; Kobayashi, J.; Kawashima, T.; Gabbai, F. P. *Chem. Commun.* **2007**, 1133. (i) Sun, Y.; Ross, N.; Zhao, S. B.; Huszarik, K.; Jia, W. L.; Wang, R. Y.; Wang, S. *J. Am. Chem. Soc.* **2007**, *129*, 7510. (j) Jäkle, F. *Coord. Chem. Rev.* **2006**, *250*, 1107. (k) Wang, S. *Coord. Chem. Rev.* **2001**, *215*, 79. (l) Elbing, M.; Bazan, G. C. *Angew. Chem., Int. Ed.* **2008**, *47*, 834.

(2) (a) Noda, T.; Shirota, Y. *J. Am. Chem. Soc.* **1998**, *120*, 9714. (b) Shirota, Y. *J. Mater. Chem.* **2005**, *15*, 75. (c) Noda, T.; Ogawa, H.; Shirota, Y. *Adv. Mater.* **1999**, *11*, 283. (d) Shirota, Y.; Kinoshita, M.; Noda, T.; Okumoto, K.; Ohara, T. *J. Am. Chem. Soc.* **2000**, *122*, 1102. (e) Jia, W. L.; Bai, D. R.; McCormick, T.; Liu, Q. D.; Motala, M.; Wang, R.; Seward, C.; Tao, Y.; Wang, S. *Chem.—Eur. J.* **2004**, *10*, 994. (f) Wakamiya, A.; Mori, K.; Yamaguchi, S. *Angew. Chem., Int. Ed.* **2007**, *46*, 4273. (g) Sundararaman, A.; Venkatasubbaiah, K.; Victor, M.; Zakharov, L. N.; Rheingold, A. L.; Jäkle, F. *J. Am. Chem. Soc.* **2006**, *128*, 16554. (h) Jia, W. L.; Feng, X. D.; Bai, D. R.; Lu, Z. H.; Wang, S. *Chem. Mater.* **2005**, *17*, 164. (i) Welch, G. C.; Juan, R. S.; Masuda, J. D.; Stephan, D. W. *Science* **2006**, *314*, 1124.

(3) (a) Wakamiya, A.; Taniguchi, T.; Yamaguchi, S. *Angew. Chem., Int. Ed.* **2008**, *47*, 834. (b) Liu, Q. D.; Mudadu, M. S.; Thummel, R.; Tao, Y.; Wang, S. *Adv. Funct. Mater.* **2005**, *15*, 143. (c) Liu, S. F.; Wu, Q.; Schmider, H. L.; Aziz, H.; Hu, N. X.; Popovíc, Z.; Wang, S. *J. Am. Chem. Soc.* **2000**, *122*, 3671. (d) Wu, Q.; Esteghamatian, M.; Hu, N. X.; Popovic, Z.; Enright, G.; Breeze, S.; Wang, S. *Angew. Chem. Int. Ed* **1999**, *38*, 985. (e) Chen, H. Y.; Chi, Y.; Liu, C. S.; Yu, J. K.; Cheng, Y. M.; Chen, K. S.; Chou, P. T.; Peng, S. M.; Lee, G. H.; Carty, A. J.; Yeh, S. J.; Chen, C. T. *Adv. Funct. Mater.* **2005**, *15*, 567. (f) Hoefelmeyer, J. D.; Schulte, M.; Tschinkl, M.; Gabbai, F. P. *Coord. Chem. Rev.* **2002**, *235*, 93.

(4) (a) Wrackmeyer, B. *Annu. Rep. NMR Spectrosc.* **1988**, *20*, 61. (b) Claridge, T. D. W. *High Resolution NMR Techniques in Organic Chemistry*, Pergamon Press: Oxford, U.K., 1999. (c) Williams, D. H.; Fleming, I. *Spectroscopic Methods in Organic Chemistry*, 4th ed.; McGraw-Hill: London, 1987.

(5) (a) Wilkey, J. D.; Schuster, G. B. *J. Org. Chem.* **1987**, *52*, 2117. (b) Wilkey, J. D.; Schuster, G. B. *J. Am. Chem. Soc.* **1988**, *110*, 7569.

(6) (a) Eisch, J. J.; Galle, J. E. *J. Am. Chem. Soc.* **1975**, *97*, 4436. (b) Eisch, J. J.; Galle, J. E.; Shafii, B.; Rheingold, A. L. *Organometallics* **1990**, *9*, 2342. (c) Eisch, J. J.; Shah, J. H.; Bolesklawski, M. P. *J. Organomet. Chem.* **1994**, *464*, 11. (d) Pelter, A.; Pardasani, R. T.; Pardasani, P. *Tetrahedron* **2000**, *56*, 7339.

(7) (a) Ashe, A. J., III.; Drone, F. J. *J. Am. Chem. Soc.* **1987**, *109*, 1879. (b) Ashe, A. J., III.; Drone, F. J.; Kausch, C. M.; Kroker, J.; Al-Taweel, S. M. *Pure Appl. Chem.* **1990**, *62*, 513. (c) Ashe, A. J., III.; Klein, W.; Rousseau, R. *Organometallics* **1993**, *12*, 3225. (d) Schulman, J. M.; Disch, R. L. *Organometallics* **2000**, *19*, 2932. (e) Schulman, J. M.; Disch, R. L.; Sabio, M. L. *J. Am. Chem. Soc.* **1982**, *104*, 3785. (g) Sugihara, Y.; Miyatake, R.; Murata, I.; Imamura, A. *Chem. Commun.* **1995**, 1249.

(8) *Photochromism: Molecules and Systems*, 2nd ed.; Dürr, H., Bouas-Laurent, H., Eds.; Elsevier, Amsterdam: The Netherlands, 2003; and references therein.

JA8052046